Ionic Strength Dependence of the Second Virial Coefficient of Low Molar Mass DNA Fragments in Aqueous Solutions

Taco Nicolai and Michel Mandel*

Department of Physical and Macromolecular Chemistry, Gorlaeus Laboratories, Leiden University, P.O. Box 9502, 2300 RA Leiden, The Netherlands. *Received March 18, 1988; Revised Manuscript Received June 13, 1988*

ABSTRACT: Second virial coefficients of low molar mass DNA fragments of approximately 150 base pairs (molar mass approximately 10^5 g mol^{-1}) have been determined with the help of static low-angle laser light scattering at seven different NaCl concentrations (ranging from 0.002 to 0.5 M) in aqueous solutions. The value of A_2 is found to decrease with increasing salt concentration. The experimental values of A_2 are compared to theoretical ones calculated for uniformly charged rigid rods. The agreement is satisfactory if the structural linear charge density is replaced in the theoretical expressions, based on line charges, by an effective value for which several approaches have been used, including the condensation concept and the (approximate) solution of the Poisson Boltzmann equation. Best results are obtained if a salt concentration independent value of the effective charge density, slightly larger than the value predicted by the simple condensation hypothesis, is used. These results seem to confirm that the DNA fragments with a contour length of the same order as (or smaller than) the total persistence length behave to a good approximation as rodlike particles.

Introduction

Low molar mass DNA is a highly charged, more or less rigid macromolecule and may therefore be suitable for studying the electrostatic interaction between highly charged cylindrical particles in a solution containing salt. Several authors have derived expressions to describe the electrostatic interaction between rodlike polyelectrolytes.[1-5] In these theories the polyion is modeled as an infinite line charge. The electrostatic interaction is then calculated within the Debye–Hückel approximation. Fixman and Skolnick have compared their theory with experiments on poly(acrylic acid).[3] They have concluded that the agreement between theory and experiment is good, although there remains some uncertainty as to the effect of chain flexibility. No comparison between theory and experiments with highly charged rodlike polyelectrolytes exists to our knowledge, however.

A very direct comparison between theory and experiment is obtained through the second virial coefficient. Experimental values of the second virial coefficient may be compared with theoretical values in which electrostatic interaction between highly charged cylinders has been incorporated. Usually in the derivation of the theoretical expression for the second virial coefficient it is assumed that the polyelectrolytes are very long. It is therefore necessary to estimate the influence of end effects if low molar mass DNA is used to compare experimental results with the theory.

When testing the validity of theoretical expressions of the second virial coefficient, it is necessary to measure the influence of the salt concentration on the second virial coefficient, because the electrostatic interaction is to a high degree influenced by the ionic strength of the solution. Static low-angle laser light scattering (LALLS) has been used to determine the second virial coefficient of short DNA fragments (150 base pairs) at various NaCl concentrations. If the persistence length of DNA has approximately the same value as the contour length of the fragments (50 nm) or is larger, depending on the salt concentration, the fragments may be expected to behave as near rodlike particles.[6] The LALLS technique has the advantage of giving direct information on the molar mass and the second virial coefficient.

The purpose of the present article is to compare these experimental results with theoretical expressions, it will be shown that the dependence of the second virial coefficient on the salt concentration of the solution is well described by the theory, though some quantitative differences occur, depending on the choice of the effective charge density of the polyelectrolytes.

Theory

From the McMillan–Mayer theory applied to solutions of rigid macromolecules the following expression for the second virial coefficient A_2 can be derived:[7]

$$A_2 = \tfrac{1}{2}N_{Av}M^{-2}\beta \tag{1}$$

where N_{Av} is Avogadro's number, M is the molar mass of the macromolecule, and β is the effective volume excluded by one molecule for another. For uncharged rigid rodlike macromolecules, eq 1 can be put in the following form:[7-9]

$$A_2 = \pi N_{Av}d^2LM^{-2}f \tag{2a}$$

where L is the length of the macromolecule, d is the diameter, and f is a shape factor which for a rodlike particle may be written as

$$f = \tfrac{1}{4}Ld^{-1}\left\{1 + \left(\frac{3+\pi}{2}\right)dL^{-1} + \frac{\pi}{4}d^2L^{-2}\right\} \tag{2b}$$

Here only *hard-core interactions* are taken into account, which means that the potential of mean force between two rods becomes infinite whenever the two molecules overlap and vanishes elsewhere. For thin rods ($L \gg d$) the expression for the second virial coefficient becomes

$$A_2 \simeq \tfrac{1}{4}\pi M^{-2}N_{Av}L^2d \tag{3}$$

For highly charged rodlike macromolecules, it is assumed that if the separation between the particles is larger than their diameter, electrostatic interactions dominate all other interactions. Thus in a first approximation the total excluded volume can be viewed as the sum of a hard-core part (β_c) and an electrostatic part (β_e)

$$\beta = \beta_e + \beta_c \tag{4}$$

For $L \gg d$, the electrostatic part of the excluded volume may be written as[3]

$$\beta_e = 2L^2\int_0^{\pi}\sin\theta\int_d^{\infty}(1 - \exp[-w_e/k_BT])\,dx\,d\theta \tag{5}$$

Here w_e is the electrostatic potential of mean force between two macromolecules in the given "solvent", k_B is the Boltzmann constant, T is the absolute temperature, x is the shortest distance between the two particles, and θ is the angle between their axes.

0024-9297/89/2222-0438$01.50/0

An exact expression for this potential of mean force between two charged rigid rodlike particles of finite thickness is not yet available. The difficulties for obtaining such an expression are directly related to those of calculating the mean electrostatic potential around such particles in a solution containing low molar mass electrolyte. As proposed by Brenner and Parsegian[1] the rodlike particles may be replaced by a line charge with an effective linear charge density different from that of the original rod, and for the potential ψ the solution of the *linearized* Poisson–Boltzmann equation of the line charge may be used. In this approximation the reduced electrostatic potential ϕ_L is given by

$$\phi_L = q\psi/k_BT = 2\nu_{eff}QK_0(\kappa r) \quad (6)$$

Here K_0 is the zero-order modified Bessel function, q is the charge of the proton, ν_{eff} is the number of elementary charges per unit length, r the radial distance from the line charge, and Q the Bjerrum length defined by the following expression for a solvent of relative permittivity ϵ.

$$Q = q^2/\epsilon k_BT \quad (7)$$

The Debye screening length κ^{-1} is given by

$$\kappa^{-1} = (8\pi Q\rho_s)^{-1/2} \quad (8)$$

with ρ_s the concentration (in particles per unit volume) of mono-monovalent salt.

The effective charge density of the hypothetical line charge is chosen in such a way that ϕ_L matches the potential around the real polyion at distance from the chain sufficiently large for $\phi \ll 1$ due to screening by the small ions. The electrostatic interaction between two cylindrically symmetric polyelectrolyte rods can thus be modeled by that between two equivalent line charges within the Debye–Hückel approximation using the effective linear charge density.

$$w_e/k_BT \simeq 2\pi\nu_{eff}^2Q \exp(-\kappa r)(\sin\theta)^{-1} = w'_e/k_BT \quad (9)$$

Use in eq 5 of the approximate expression w'_e, valid strictly speaking only under conditions for which $\phi \ll 1$, is reasonable because the main contribution of w_e to the integral in eq 5 refers to distances where w_e is not large compared to k_BT. At smaller distances the error due to replacing w_e by w'_e decrease exponentially with $(w_e - w'_e)/k_BT$.

Combination of eq 5 and 9 yields the following approximate expression for the electrostatic contribution to the excluded volume.[3]

$$\beta_e = (\pi/2)L^2\kappa^{-1}(\ln Y + \gamma - \tfrac{1}{2} + \ln 2) \quad (10a)$$

with

$$Y = 2\pi\nu_{eff}^2Q\kappa^{-1} \exp(-\kappa d) \quad (10b)$$

where γ denotes Euler's constant ($\gamma = 0.577\,21$). Equation 10 is accurate within 2% for $Y > 2$. Combining eq 4, 5, and 10 the following expression of the excluded volume is obtained for $L \gg d$:

$$\beta = (\pi/2)L^2[d + \kappa^{-1}(\ln Y + \gamma - \tfrac{1}{2} + \ln 2)] \quad (11)$$

which is equivalent to the excluded volume due to the hard-core interactions of uncharged rigid rods with an effective diameter

$$d_{eff} = d + \kappa^{-1}(\ln Y + \gamma - \tfrac{1}{2} + \ln 2) \quad (12)$$

If the salt concentration of the solution and the dimensions of the polyion are known, the only unknown parameter necessary for the calculation of the excluded volume is ν_{eff}. The effective charge density is obtained by matching the potential around the real polyion with the potential around the hypothetical line charge for distances large compared to the Debye–Hückel screening length.

There are two fundamentally different approaches to describe the potential around a highly charged cylindrical macromolecule. One way is to solve the Poisson–Boltzmann equation by using appropriate boundary conditions. The other is the counterion condensation approach developed by Manning[10] where, again, the real macromolecule is replaced by a line charge with a potential in the linearized limit and with an effective charge parameter ζ_{eff}, depending on the value of the real linear charge density of the macromolecule and the corresponding charge parameter $\zeta = \nu Q$ (with ν the number of elementary charges per unit contour length). The reduction of the charge parameters is due to condensation of counterions in the close neighborhood of the macromolecule.

$$\zeta_{eff} = \nu Q \qquad \nu Q \le 1 \quad (13)$$
$$\zeta_{eff} = 1 \qquad \nu Q > 1$$

A review of both approaches is given by Anderson and Record.[11]

We have used both ways to determine ν_{eff} necessary in the calculation of the excluded volume and effective diameter according to eq 11 and 12, respectively.

In the first, the expression for the linearized solution of the Poisson–Boltzmann equation of a cylindrical uniformly charged macromolecule of radius a, valid at distances sufficiently large with respect to the Debye–Hückel screening length, is used

$$\phi_L = \frac{2\zeta K_0(\kappa r)}{\kappa a K_1(\kappa a)} \quad (14)$$

but with ζ in eq 14 replaced by ζ_{eff} according to the condensation rule, eq 13.[12] Here K_1 is the first-order modified Bessel function By comparison of eq 14, with ζ_{eff} replacing ζ, with eq 6, the effective charge density is given by the following expression valid for $\nu Q > 1$, as for DNA in aqueous solutions at 25 °C $\nu Q = 4.3$, taking 0.33 nm as the rise per base pair of the double helix.

$$\nu_{eff} = [Q\kappa a K_1(\kappa a)]^{-1} \quad (15)$$

Here $[\kappa a K_1(\kappa a)]^{-1}$ constitutes a correction due to the finite radius of DNA and the influence of the ionic strength of the solution. If in eq 15 the radius a tends to zero, we obtain Manning's result as

$$\lim_{\kappa a \to 0} \kappa a K_1(\kappa a) = 1 \quad (16)$$

Therefore another possibility for applying the condensation approach is to use $\nu_{eff} = Q^{-1}$ as follows directly from eq 13 for the case $\nu Q > 1$. This values of ν_{eff} would be independent of the ionic strength, however.

In the other approach we need the solution of the Poisson–Boltzmann equation around a cylindrical macromolecule in the presence of low molar mass salt. An analytical solution has not yet been found, but the equation may be solved numerically or analytical approximations may be used. Here we applied the approximate expressions obtained by Philip and Wooding,[13] which have been found to correspond within a few percent to the results obtained from the numerical solution of the Poisson–Boltzmann equation. For distances from the polyion large compared to the Debye–Hückel screening length, the potential becomes proportional to a zero-order modified Bessel function as is the case for the solution of the linearized Poisson–Boltzmann equation.

$$\phi = BK_0(\kappa r) \qquad (r > a + \kappa^{-1}) \quad (17)$$

To match the potential around the cylindrical polyelectrolyte with the potential around the hypothetical line

charge, the effective linear charge density in eq 6 has to be chosen in such a way that

$$\nu_{eff} = B/2Q \tag{18}$$

The value of B may be obtained from the approximated solution according to Philip and Wooding for each salt concentration considered (see Appendix). Note that B must be assumed to be independent of r, a condition which has been shown to be only approximately true.[14]

Equation 11 has been derived under the condition $L \gg d$ for which end effects are negligible. For low molar mass DNA fragments this is no longer permissible, however. Skolnick and Grimmelman[15] have calculated the potential around a line charge of finite length within the Debye–Hückel approximation. Their results show that the potential at large distances approaches the potential around a point charge and at small distances the potential around a line charge of infinite length. To what extent the latter result is valid depends on the length of the line charge and the Debye–Hückel screening length. If the length of the line charge is large compared to the Debye–Hückel screening length (as is the case in all our experiments where $L\kappa > 8$), the infinite line charge approach is valid for all distances from the line charge where the potential is not negligible.

Katoh and Ohtsuki[16] have solved numerically the Poisson–Boltzmann equation for uniformly charged cylinders with finite length. Their calculations show that end effects on the electrostatic potential extend to a distance of about $0.5\kappa^{-1}$ from the end of the cylinder. This estimate of the end-effects is approximately independent of the charge density, the diameter of the charged cylinder, and the salt concentration of the solution.

In view of these results it seems justified to incorporate end effects in the calculation of the excluded volume by using an effective length

$$L_{eff} = L + \kappa^{-1} \tag{19}$$

A rodlike polyion can thus be modeled by an uncharged cylinder with an effective diameter given by eq 12 and an effective length given by eq 19. The second virial coefficient for rods with diameter d_{eff} and length L_{eff} is (see eq 2)

$$A_2 = \tfrac{1}{4}\pi N_{AV} M^{-2} d_{eff} L_{eff}^2 \left\{1 + \frac{(3+\pi)}{2}\left(\frac{d_{eff}}{L_{eff}}\right) + \frac{\pi}{4}\left(\frac{d_{eff}}{L_{eff}}\right)^2\right\} \tag{20}$$

Materials and Methods

Sample Preparation. The low molar mass DNA used has been prepared from chicken crythrocyte DNA, obtained by the procedures described by Shindo et al.[17] The DNA was digested at 37 °C by micrococcal nuclease (Worthington Diagnostic Systems, Inc.; 3600 units) for about 1 h. The mononucleosomes were separated from smaller DNA fragments by dialysis against a solution of 0.1 M KCl, 0.05 M Tris pH 7 buffer, 10^{-4} M EDTA and 10^{-4} M phenylmethanesulfonyl fluoride. Proteins were removed by a phenol/chloroform/isoamyl alcohol extraction. The mononucleosome DNA was precipitated from the purified solution by cold alcohol (−20 °C), redissolved in water, and then dialyzed against pure water at 4 °C. After dialyzation the sample was freeze-dried and stored at −20 °C. Several isolations were performed and, usually, out of 3–6 L of chicken blood, 1–2 g of mononucleosome DNA was obtained.

Characterization by gel electrophoresis and a combination of gel permeation chromatography (GPC) and low-angle laser light scattering (LALLS) showed that the first sample obtained (sample A) was nearly homodisperse DNA with a weight-averaged molar mass of approximately 100 000 g mol^{-1}.[18] DNA obtained from subsequent preparations has been characterized by GPC. Only those samples have been used in the light scattering experiments for which the RI chromatograms where comparable to those of sample A, although small differences in average molar mass and molar mass distribution cannot be excluded.

The protein content of the samples was found by total amino acid analysis (performed at the Biochemistry Department of this university) to be negligible (less than 0.03%). Freeze-dried DNA showed no signs of denaturation in all cases, even after storage at −20 °C for more than 1 year. This has been checked by the method of Hirshman and Felsenfeld[19] and by GPC experiments.

Solutions were prepared by dissolving freeze-dried DNA into deionized and Millipore-filtered water to which NaCl of analytical grade had been added to the desired salt concentrations. All solutions were filtered through Millipore filters (0.22 μm) before use. DNA concentrations were determined spectrophotometrically at 260 nm, using an extinction coefficient of 20 dm^3 g^{-1} cm^{-1}.[17] Concentrations were always determined *after* light scattering experiments in order to account for possible losses due to filtrations.

Static Low-Angle Laser Light Scattering Experiments. LALLS experiments have been performed with a Chromatix KMX-6 apparatus operating at 633 nm and at 25.0 °C. From the excess intensity of the scattered light of the solution over that of the solvent (aqueous solution of NaCl at the same concentration) at angle θ, the so-called Rayleigh factor ΔR_θ is determined.

$$\Delta R_\theta = ((I_{C,\theta} - I_{0,\theta})/I^0)F \tag{21}$$

Here $I_{C,\theta}$ is the intensity of the light scattered by the solution of concentration C at angle θ, $I_{0,\theta}$ is the intensity of the light scattered at the same angle by the solvent only, I^0 is the intensity of the incident beam, and F is an instrumental constant. The Rayleigh factor is related to the weight-averaged molar mass M_w and the second virial coefficient of the solute by the classical expression

$$KC/\Delta R_\theta = M_w^{-1}P(\theta)^{-1} + 2A_2S(\theta)P(\theta)^{-1}C + \ldots \tag{22}$$

with

$$K = 4\pi^2 n_0^2 \lambda_0^{-4} N_{Av}^{-1} (\partial n/\partial C)_{\mu_s}^2 \tag{23}$$

The symbols $P(\theta)$ and $S(\theta)$ refer to the intramolecular and the intermolecular interference factors, respectively. Note that $P(\theta) \to 1$ and $S(\theta)/P(\theta) \to 1$ as $\theta \to 0$. Furthermore n_0 stands for the refractive index of the solvent and λ_0 for the wavelength of the incident beam in vacuum (633 nm for the experiments performed with the KMX-6). The refractive index increment $(\partial n/\partial C)_{\mu_s}$ has to be determined under conditions where the chemical potential of the salt μ_s is kept constant. At the small angle at which the measurements are performed on the KMX-6 ($\theta \leq 6°$), both $P(\theta)$ and $S(\theta)/P(\theta)$ may be set equal to unity. Thus direct information about the molar mass and the second virial coefficient A_2 is obtained from the static LALLS experiment if the refractive index increment at the same wavelength is known.

Refractive index increments of DNA have been determined at 633 nm and 25 °C with a Chromatix KMX-16 differential refractometer. Usually the same solutions were used for the determinations of the refractive index increments and for the LALLS experiments. Values of the

Table I
Comparison between Experimental and Theoretically Calculated Values of the Second Virial Coefficient A_2 of Low Molar Mass DNA at Various Salt Concentrations C_s

C_s, mol dm^{-3}	κ^{-1}, nm	$(M_w)_{exp}$, g mol^{-1} × 10^{-5}	$(A_2)_{exp}$, mol dm^3 g^{-2} × 10^6	$(A_2)_{th}$							
				ν_{eff}	$A_2^{(1)\,a}$	$A_2^{(2)\,a}$	ν_{eff}^{b}	$A_2^{(1)\,b}$	$A_2^{(2)\,b}$	$A_2^{(1)\,c}$	$A_2^{(2)\,c}$
0.5	0.44	1.00 ± 0.02	0.20 ± 0.15	(36.3)	0.6	0.6	(10.7)	0.4	0.4	0.1	0.1
0.1	0.97	1.00 ± 0.02	0.60 ± 0.15	7.5	1.0	1.1	2.9	0.7	0.7	0.4	0.4
0.04	1.54	1.11 ± 0.03	1.00 ± 0.15	4.5	1.7	1.7	2.1	1.1	1.1	0.9	0.9
0.02	2.17	1.01 ± 0.03	2.0 ± 0.2	3.4	2.6	2.7	1.8	1.8	1.9	1.6	1.6
0.01	3.07	1.32 ± 0.03	2.9 ± 0.2	2.7	4.4	3.9	1.6	3.2	2.9	2.9	2.7
0.005	4.35	1.22 ± 0.07	6.1 ± 0.2	2.3	7.7	7.2	1.5	6.0	5.6	5.7	5.3
0.002	6.87	1.02 ± 0.07	18.1 ± 0.4	1.9	18.3	19.6	1.5	15.2	16.3	15.0	16.0

[a] ν_{eff} estimated according to eq 18. [b] ν_{eff} estimated according to eq 15. [c] $\nu_{eff} = Q^{-1} \cdot A^{(1)}$ calculated with average value of L and $A^{(2)}$ calculated with different L for different values of C_s (see text).

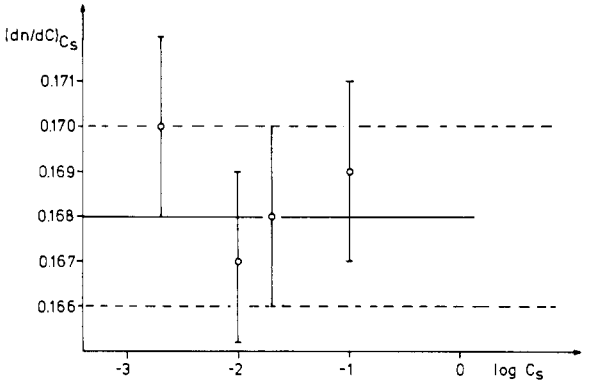

Figure 1. Refractive index increment of low molar mass DNA at different salt concentrations C_s. The full horizontal line represents the value averaged over all four C_s values; the dotted lines indicate the range corresponding to the standard deviation.

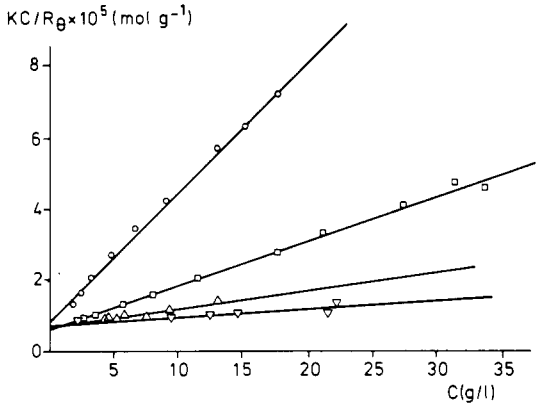

Figure 2. Variation of $KC/\Delta R_\theta$ with DNA concentration C at various salt concentrations: 0.02 M NaCl (▽); 0.01 M NaCl (▲); 0.05 M NaCl (□); 0.02 M NaCl (○). Results at very low concentrations are not shown for sake of clarity but do not deviate significantly from the different straight lines drawn.

refractive index increment have been determined at various salt concentrations between 0.002 and 0.1 M NaCl. Dialysis of the DNA samples against salt solutions of constant concentration before the measurements had no influence on the value of the refractive index increment measured. The increase of the refractive index of the solution over that of water[20] was found to be linear in DNA concentration in the whole range of concentrations explored. Values of the refractive index increments at λ_0 = 633 nm are shown in Figure 1. They are independent of the salt concentration within experimental error, in contrast to the small increase with decreasing NaCl concentration found for DNA with a higher molar mass (M_w = 3 × 10^5 g mol^{-1}, average value of dn/dC = (0.172 ± 0.005) × 10^{-3} dm^3 g^{-1}).[21] The averaged value found (0.168 ± 0.002) × 10^{-3} dm^3 g^{-1} is in agreement with values used in the literature.[21-23]

Results

The time-averaged intensity of the scattered light was always measured on solutions which were pumped continuously through the measuring cell of the Chromatix KMX-6 after passing a Millipore filter (0.22 μm). When the flow was stopped, the intensity of the light scattered from the solutions with *low* ionic strength slowly increased and fluctuated strongly. This behavior was more pronounced the higher the DNA concentration and the lower the salt concentration. Anomalous behavior of DNA solutions at low ionic strength has been observed in other experimental investigations as well.[24,25] A possible cause for this time-dependent behavior is the slow formation of small amounts of aggregates or local ordering in the solution.

The concentration dependence of the excess scattered light was determined at various salt concentrations between 0.002 M and 0.5 M NaCl. For each salt concentration the values of $KC/\Delta R_\theta$ have been plotted against the DNA concentration C (with generally 0.05 < C < 35 g dm^{-3}). The experimental points fall in a very good approximation on a straight line for the whole concentration range investigated (see Figure 2). From the slopes of these lines the second virial coefficients can be determined according to eq 22 and from the intercept the weight-averaged molar mass. Values of A_2 and M_w derived from a linear least-squares analysis of the experimental results at constant C_s have been summarized in Table I.

The values of M_w show some scattering around an average of M_w = (1.10 ± 0.13) × 10^5 g mol^{-1} with no value smaller than 10^5. There is, however, no definite trend in the change of the experimental values with decreasing C_s (see Table I). The strongest deviation with respect to the mean occurs at C_s = 0.01 M but still falls within an interval of twice the standard deviation of the mean. It cannot be excluded, on the other hand, that these fluctuations in the average molar mass may be due to variations in the different DNA samples[18]) or the problems related to complete dust removal (particular difficult in aqueous solutions). The mean value is, anyway, in agreement with the value expected for mononucleosome DNA of 150 base pairs (M = 9.9 × 10^4 g mol^{-1}). If the molar mass which deviates most from the mean is not taken into account, a new average value of M_w = (1.06 ± 0.09) × 10^5 g mol^{-1} can be derived. The latter is also in agreement with the theoretical value for 150 base pairs and is consistent with the overall mean. Even if in the case of the sample with the largest value of M_w contains some aggregates, the fraction of DNA molecules participating in the aggregates would be small. Assuming, e.g., that one would have a mixture of monomeric DNA (with molar mass 10^5 g mol^{-1}) and pentamers (with molar mass 5 × 10^5 g mol^{-1}), the mole

fraction of the former would be 0.98. There is therefore no significant indication of aggregation under the experimental conditions used.

Theoretical values of the second virial coefficients have been calculated according to eq 20 put into the following form

$$A_2 = \frac{1}{4}\pi N_{Av} M_L^{-2} d_{eff}((1 + x)^2 + (3 + \pi)(1 + x)y + \pi y^2) \quad (20a)$$

$$x = \kappa^{-1}/L \quad (20b)$$

$$y = (d_{eff}/2L) \quad (20c)$$

In the calculations the structural diameter of DNA was taken equal to 2.5 nm and the rise per base pair equal to 0.33 nm[26]). These values yield a molar mass per unit length M_L = 1950 g mol^{-1} nm^{-1} and a number of elementary charges per unit length of ν = 6.1 nm^{-1} (assuming two negative charges per base pair originating from the phosphate groups). The value of d_{eff} has been calculated according to eq 12 by using for the effective charge density ν_{eff} three different estimates. These were the values predicted by eq 15 and 18 and by $\nu_{eff} = Q^{-1}$. For κ^{-1} the values given in Table I have been used. They have been calculated with eq 8, thus neglecting the contributions to the ionic strength which may arise, at higher DNA concentrations, from the Na^+ ions provided by the polyelectrolyte. This seems permissible as no significant changes in the linearity of $(KC/\Delta R_0)C$ vs C at constant C_s has been observed at high values of C. For each choice of ν_{eff} two sets of A_2 values have been calculated. In the first a single constant length L of the DNA was used, calculated from M_L and the experimentally determined average M_w = 1.1 × 10^5 g mol^{-1} ($A_2^{(1)}$); in the second a different value of L has been used at each salt concentration, calculated with the experimental value of M_w at the given C_s and M_L ($A_2^{(2)}$). These different values are compared to the experimentally determined second virial coefficients in Table I.

Discussion

Table I clearly demonstrates the ionic strength dependence of A_2. There is a large increase of $(A_2)_{exp}$ with decreasing salt concentration. This increase must be primarily determined by the increase of the electrostatic interactions, i.e., the electrostatic repulsions between the DNA molecules. From Table I it can also be seen that the calculated values of A_2 according to eq 20 are of the right order of magnitude and show the same trend with decreasing C_s as the experimental values, irrespective of the choice ν_{eff} or L (Figure 3). It can be observed that the calculated values of A_2 are even in satisfactory agreement with the experimental ones for ν_{eff} obtained by the condensation approach, i.e., either through eq 15 or by assuming $\nu_{eff} = Q^{-1}$, except for the lowest salt concentration. There is no indication whether a constant value of L or a variable one is to be preferred. The use of eq 15 instead of taking the straightforward condensation value Q^{-1} for the effective charge density for the highly charged DNA molecule does not seem to make any significant difference for the calculated values of A_2 with respect to the experimental value, except at the highest salt concentration where the second virial coefficient is already very small.

The values of ν_{eff} obtained through the Poisson–Boltzmann approach, eq 18, seem to lead systematically to higher values of A_2 as compared to the experimental ones, except at the lowest salt concentration where the agreement is even better than for the values calculated by the condensation approach. These systematically higher values

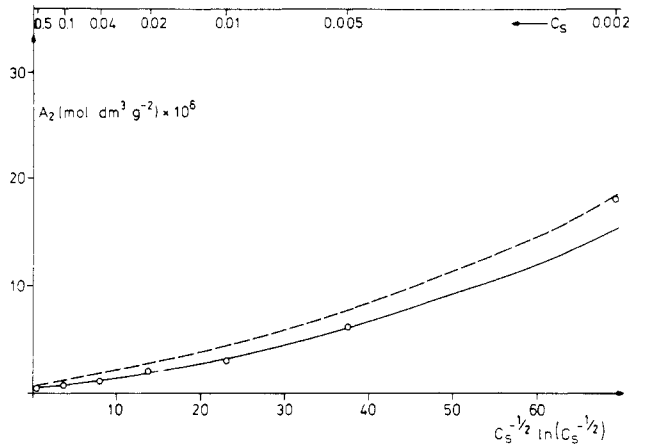

Figure 3. Variation of the second virial coefficient with $C_s^{-1/2}$ ln ($C_s^{-1/2}$) (proportional to κ^{-1} ln κ^{-1}). The circles represent the experimental values; the full curve and the dashed one represent the theoretical variation of $A_2^{(1)}$ calculated with ν_{eff}, according to eq 15 and 18, respectively.

are not attributable to an overestimation of end effects. If in the calculation according to eq 20 the effective lengths are lowered in comparison to the structural length, i.e., x = 0, the calculated values of the second virial coefficient decreases only slightly. On the other hand in these calculations it has been assumed that DNA dissociates completely in water and that each phosphate group carries one elementary charge. Schellman and Stigter have suggested from electrophoretic data that the charge density of DNA is lower and amounts to a charge of $-0.73q$ per phosphate group[27] due to the binding of Na^+ inside the helix (not to be confused with counterion condensation). Use of this reduced charge density in the calculation according to the Poisson–Boltzmann approach reduces the estimated values of A_2 to an extent of only 5–10%.

Another uncertainty in these calculations is the diameter of DNA in water. Reducing it from 2.5 to 2.0 nm lowers the theoretically calculated value of A_2 merely a few percent. The uncertainties in the values of these three parameters are unable to explain therefore why, except at C_s = 0.002 M, the theoretically calculated values of A_2 using the Poisson–Boltzmann approach are systematically above the experimental ones but exhibit qualitatively the same salt concentration dependence.

From the experimental A_2 values, effective charge densities may be obtained by iteration using eq 12 and 20. Interestingly enough, these values fluctuate strongly around a mean of 1.8 ± 0.3 (see Figure 4), whether one uses a constant or a variable value for L. Theoretical values of A_2 from this value of ν_{eff} give very satisfactory agreement with experimental values (see Figure 5), in fact a better fit than with any of the three other sets of ν_{eff} values that can be predicted theoretically.

It follows from this analysis that for the low molar mass DNA fragments and the experimental conditions used, the second virial coefficients as measured are consistent with those for a rodlike, uniformly charged macromolecule, provided an effective charge density smaller than the structural value is used. A constant value for the whole ionic strength range explored is also predicted by a simple condensation approach and yields quite acceptable values for A_2, albeit not as good as a value ν_{eff} somewhat higher than Q^{-1}. It is not very clear why a constant value of ν_{eff}, instead of a salt concentration dependent one as predicted from the Poisson–Boltzmann approach, is in this context satisfactory. Given the crudeness of the model used, this is most likely due to a compensation of errors. It should not be forgotten that several severe approximations have

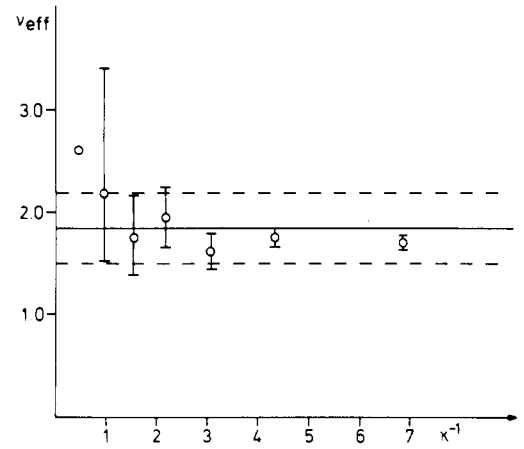

Figure 4. Effective charge densities ν_{eff} derived from experimental A_2 values with the help of eq 12 and 20. The error bars correspond to the inaccuracy on A_2. The horizontal full line corresponds to the average value of ν_{eff}; the dashed lines indicate the range corresponding to the standard deviation.

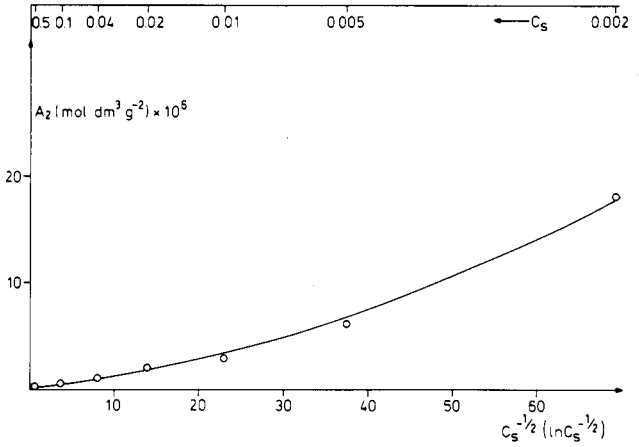

Figure 5. Comparison between the experimental values of A_2 (circles) and the theoretical variation of A_2 with salt concentration according to eq 20, using ν_{eff} = 1.84.

been used in the theoretical calculation of the second virial coefficient, such as the use of a line charge compensated by the use of an effective charge density and a local Debye–Hückel potential (which is in itself a solution for a linearized Poisson–Boltzmann equation). A more rigorous theoretical treatment for the second virial coefficient of (rodlike) polyelectrolytes is still badly needed and will hopefully become available in the near future. It does not affect the conclusion, however, that the DNA molecules studied behave to a good approximation as rodlike particles, in good agreement with expectations based on a wormlike chain approach for polyelectrolytes.[21,28-30]

In Table I the values of ν_{eff} estimated through eq 15 and 18 for the highest salt concentrations C_s = 0.5 have been put between brackets because these values are too high to have any physical significance. At this high salt concentration, where κ^{-1} is rather small, the principles on which the estimations have been based probably break down. Note that these high values for the effective charge density barely affect the values of the calculated A_2, however. In fact at the high salt concentration considered (C_s = 0.5 M) a calculation of the second virial coefficient according to eq 2 *without* any correction for the diameter and the length of DNA would yield a value $A_2 = 0.3 \times 10^{-6}$ mol dm^3 g^{-2}, which is in good agreement with the experimental result.

Finally we have represented in Figure 6 the change of the effective diameter, d_{eff}, calculated according to eq 12, with the salt concentration for the different sets of values

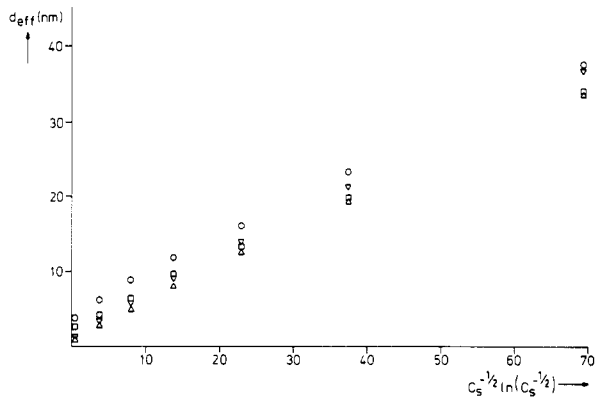

Figure 6. The variation of d_{eff} with salt concentration. Different symbols correspond to different estimates for ν_{eff}: (○) ν_{eff} according to eq 18; (□) ν_{eff} according to eq 15; (△) ν_{eff} = 1.43; (▽) ν_{eff} = 1.84.

ν_{eff} used. It may be seen that this effective diameter increases with decreasing salt concentration to values which are considerably higher than κ^{-1} (see Table I), the zero-order correction for d_{eff} as compared to d.[30]

Acknowledgment. These investigations have been carried out under the auspices of the Netherlands Foundation for Chemical Research (SON) and with financial aid from the Netherlands Organization for the Advancement of Pure Research (ZWO).

Appendix

Calculation of the Effective Charge Density from an Approximated Analytical Solution of the Poisson–Boltzmann Solution. The Poisson–Boltzmann equation for cylindrical polyions in the presence of monovalent counter- and coions of practically equal concentrations is given by

$$R^{-1}\left(\frac{d}{dR}\right)\left[R\left(\frac{d\phi}{dR}\right)\right] = \sinh \phi \qquad \text{(A.1)}$$

with $R = \kappa r$. This equation cannot be solved analytically. Therefore Philip and Wooding[13] used approximated equations for two different regions of R:

$$R^{-1}\left(\frac{d\phi}{dR}\right)\left[R\left(\frac{d\phi}{dR}\right)\right] = \tfrac{1}{2}\exp(\phi) \qquad R \le R^* \qquad \text{(A.2a)}$$

$$R^{-1}\left(\frac{d}{dR}\right)\left[R\left(\frac{d\phi}{dR}\right)\right] = \phi \qquad R \ge R^* \qquad \text{(A.2b)}$$

where R^* is the R value that separates the inner region governed by eq A.2a from the outer region governed by eq A.2b. R^* is defined in such a way that $\phi = 1$ at $R = R^*$. Equation A.2a expresses the fact that in the inner region the presence of coions may be neglected and eq A.2b that in the outer region a linearized equation is applicable. The solution for the outer region is

$$\phi = K_0(R)/K_0(R^*) = B(R^*)K_0(R) \qquad R \ge R^* \qquad \text{(A.3)}$$

Because ϕ must be a continuous function over both regions, the solutions of the inner region must satisfy the following conditions:

$$(\phi)_{R=R^*} = 1 \qquad \left(\frac{d\phi}{dR}\right)_{R=R^*} = -K_1(R^*)/K_0(R^*) \qquad \text{(A.4)}$$

Philip and Wooding give the solution of the Poisson–Boltzmann equation for ϕ and $d\phi/dR$ in the inner region in the form of five different equations corresponding to different values/ranges of value for R^*. The value of R^*

depends itself on the salt concentration of the solution. In the case of the low molar mass DNA fragments and the salt concentration used in the present investigation, only two of these equations are needed. There are, for $d\phi/dR$

$$d\phi/dR = -(2/R)\{1 - \tfrac{1}{2}\alpha \cot [\tfrac{1}{2}\alpha \ln (R^*/R) + \sin^{-1} (\alpha/e^{1/2}R^*)]\}$$
$$2 \times 10^{-3} \le C_s \le 2 \times 10^{-2} \text{ mol dm}^{-3} \quad \text{(A.5a)}$$

$$d\phi/dR = -(2/R)\{1 + \tfrac{1}{2}\alpha \cot [\tfrac{1}{2}\alpha \ln (R/R^*) + \sin^{-1} (\alpha/e^{1/2}R^*)]\}$$
$$4 \times 10^{-2} \le C_s \le 5 \times 10^{-1} \text{ mol dm}^{-3} \quad \text{(A.5b)}$$

In these equations e is the base of natural logarithms (e = 2.718 28). Note that for (A.5a) R^* must satisfy the condition $0.601\,973 < R^* < 1.552\,651$ and for (A.5b) $R^* > 1.552\,651$. The value of the parameter α can be related to that of R^* through the second condition (A.4).

$$\alpha = \pm\{eR^{*2} - (2 - \{R^*K_1(R^*)/K_0(R^*)\})\}^{1/2} \quad \text{(A.6)}$$

Equations for the derivatives of ϕ have been used here because the value for $d\phi/dR$ at the surface of the polyelectrolyte may be calculated from the surface charge density by using Gauss's law. At the surface where $R = R_0 = \kappa a$

$$(d\phi/dR)_{R=R_0} = -Q\nu/\kappa a \quad \text{(A.7)}$$

Values of R^* may be calculated in an iterative way by using either (A.5a) or (A.5b). Once R^* is known, ν_{eff} may be calculated from eq 17 with $B^{-1} = K_0(R^*)$.

References and Notes

(1) Brenner, S. L.; Parsegian, A. V. *Biophys. J.* **1976**, *17*, 327.
(2) Stigter, D. *Biopolymers* **1977**, *16*, 1435.
(3) Fixman, M.; Skolnick, J. *Macromolecules* **1978**, *11*, 863.
(4) Stroobants, A.; Lekkerkerker, H. N. W.; Odijk, T. *Macromolecules* **1986**, *19*, 2232.
(5) Onsager, L. *Ann. N.Y. Acad. Sci.* **1949**, *51*, 627.
(6) Elias, J. G.; Eden, D. *Macromolecules* **1981**, *14*, 410.
(7) Yamakawa, A. *Modern Theory of Polymer Solutions*; Harper & Row: New York, 1971.
(8) Tsihara, A. *J. Chem. Phys.* **1950**, *18*, 1446.
(9) Isihara, A.; Hayashida, T. *J. Phys. Soc. Jpn.* **1951**, *6*, 40.
(10) Manning, G. S. *J. Chem. Phys.* **1969**, *51*, 924.
(11) Anderson, C. F.; Record, M. T. *Annu. Rev. Phys. Chem.* **1970**, *33*, 191.
(12) Ramanathan, G. V.; Woodbury, C. P. *J. Chem. Phys.* **1982**, *77*, 4133.
(13) Philip, J. R.; Wooding, R. A. *J. Chem. Phys.* **1970**, *52*, 953.
(14) Fixman, M. *J. Chem. Phys.* **1979**, *70*, 4995.
(15) Skolnick, J.; Grimmelman, E. K. *Macromolecules* **1980**, *13*, 335.
(16) Katoh, T.; Ohtsuki, T. *J. Polym. Sci., Polym. Phys. Ed.* **1982**, *20*, 2167.
(17) Shindo, H.; Mc Ghee, J. P.; Cohen, J. S. *Biopolymers* **1980**, *19*, 523.
(18) Nicolai, T.; van Dijk, L.; van Dijk, J. A. P. P.; Smit, J. A. M. *J. Chromatogr.* **1987**, *389*, 286.
(19) Hirshman, S. Z.; Felsenfeld, G. *J. Mol. Biol.* **1986**, *16*, 347.
(20) Mandel, M.; Varkevisser, F. A.; Bloys van Treslong, C. J. *Macromolecules* **1982**, *15*, 675.
(21) Mandel, M.; Schouten, J. *Macromolecules* **1980**, *13*, 1247.
(22) Mandelkern, M.; Dattagupta, N.; Crothers, D. M. *Proc. Natl. Acad. Sci. U.S.A.* **1981**, *87*, 4294.
(23) Vreugdenhil, Th.; van der Touw, F.; Mandel, M. *Biophys. Chem.* **1979**, *10*, 67.
(24) Fulmer, A. W.; Benbasat, J. A.; Bloomfield, V. A. *Biopolymers* **1981**, *20*, 1147.
(25) Härd, T.; Kearns, D. R. *Biopolymers* **1986**, *25*, 1519.
(26) Elias, J. G.; Eden, D. *Biopolymers* **1981**, *20*, 2369.
(27) Schellman, J. A.; Stigter, D. *Biopolymers* **1977**, *16*, 1415.
(28) Odijk, T. *J. Polym. Sci., Polym. Phys. Ed.* **1977**, *15*, 477.
(29) Skolnick, J.; Fixman, M. *Macromolecules* **1977**, *10*, 944.
(30) Odijk, T.; Houwaart, A. C. *J. Polym. Sci., Polym. Phys. Ed.* **1978**, *16*, 627.

Kinetics of Isothermal Crystallization and Curie Transition of the 81/19 mol % Vinylidene Fluoride–Tetrafluoroethylene Copolymer

Hervé Marand* and Richard S. Stein

Polymer Research Institute, University of Massachusetts, Amherst, Massachusetts 01003.
Received February 27, 1988; Revised Manuscript Received June 28, 1988

ABSTRACT: The kinetics of crystallization and Curie transition of the 81/19 mol % vinylidene fluoride–tetrafluoroethylene (VF_2–F_4E) copolymer are investigated for different isothermal conditions by wide-angle X-ray diffraction, small-angle light scattering, and differential scanning calorimetry. The results of this study indicate that, in agreement with previous investigations, the isothermal crystallization from the melt produces first the paraelectric crystal phase. The paraelectric phase is observed to undergo isothermally a crystal–crystal transition into the ferroelectric phase. Examination of the melting behavior of samples crystallized for different lengths of time indicates that the ferroelectric phase does not undergo any crystal–crystal transition upon heating, as was suggested by other investigators, but melts at a temperature about 10 deg higher than the original paraelectric phase. The crystallization and crystal–crystal transition kinetics are extremely temperature dependent and the ratio of the crystallization rate to Curie transition rate increases with crystallization temperature.

Introduction

Considerable work has been carried out in the past few years to investigate the existence and characteristics of the Curie transition in poly(vinylidene fluoride) (PVF_2) and related copolymers.[1-28] The intrinsic ferroelectric nature of PVF_2 was first suggested by the observation of a ferro- to paraelectric transition in vinylidene–trifluoroethylene copolymers (VF_2–F_3E) of various VF_2 mole fractions.[1-17] Lovinger et al.[7,8] proposed a value of 205 °C for the Curie temperature of PVF_2 by extrapolation of X-ray and dielectric data for VF_2–F_3E copolymers to 100% VF_2 content. To avoid any ambiguity in the interpretation of the data as a result of the alteration of the chemical structure of PVF_2 by a different chemical species (F_3E) (difference in

* To whom correspondence should be addressed at Virginia Polytechnic Institute and State University, Chemistry Department, Blacksburg, VA 24061.

0024-9297/89/2222-0444$01.50/0